HHS Public Access

Author manuscript

Circ Res. Author manuscript; available in PMC 2016 August 14.

Published in final edited form as:

Circ Res. 2015 August 14; 117(5): 424–436. doi:10.1161/CIRCRESAHA.114.305393.

Angiotensin II Induces Skeletal Muscle Atrophy by Activating TFEB-Mediated *MuRF1* Expression

Philipp Du Bois[1], **Cristina Pablo Tortola**[1], **Doerte Lodka**[1], **Melanie Kny**[1], **Franziska Schmidt**[1], **Kunhua Song**[3,2], **Sibylle Schmidt**[1], **Rhonda Bassel-Duby**[3], **Eric N. Olson**[3], and **Jens Fielitz**[1,4]

[1]Department of Molecular Cardiology, Experimental and Clinical Research Center (ECRC), a Cooperation between Max-Delbrück-Centrum and Charité Universitätsmedizin Berlin, Campus Buch, Berlin, Germany

[3]Department of Molecular Biology, University of Texas Southwestern Medical Center, Dallas, Texas, USA

[4]Department of Cardiology, Charité Universitätsmedizin Berlin, Campus Virchow, Berlin, Germany

Abstract

Rationale—Skeletal-muscle wasting with accompanying cachexia is a life threatening complication in congestive heart failure (CHF). The molecular mechanisms are imperfectly understood, although an activated renin-angiotensin aldosterone system (RAAS) has been implicated. Angiotensin (Ang) II induces skeletal muscle atrophy in part by increased muscle-enriched E3 ubiquitin ligase muscle RING-finger-1 (*MuRF1*) expression, which may involve protein kinase-D 1 (PKD1).

Objective—To elucidate the molecular mechanism of Ang II-induced skeletal muscle wasting.

Methods and Results—A cDNA expression screen identified the lysosomal hydrolase-coordinating transcription factor EB (TFEB) as novel regulator of the human *MuRF1*-promoter. TFEB played a key role in regulating Ang II-induced skeletal muscle atrophy by transcriptional control of *MuRF1* via conserved E-box elements. Inhibiting TFEB with siRNA prevented Ang II-induced *MuRF1* expression and atrophy. The histone deactylase-5 (HDAC5), which was directly bound to and colocalized with TFEB, inhibited TFEB-induced *MuRF1* expression. The inhibition of TFEB by HDAC5 was reversed by PKD1, which was associated with HDAC5 and mediated its

Address correspondence to: Dr. Jens Fielitz, Experimental and Clinical Research Center, Lindenberger Weg 80, 13125 Berlin, Germany, Te;: +49 30 450 540424, Fax: +49 30 450 540928, jens.fielitz@charite.de.

[2]Current address: Department of Medicine, Division of Cardiology, Charles C. Gates Center for Regenerative Medicine and Stem Cell Biology, University of Colorado, Anschutz Medical Campus, Denver, USA

The authors are not aware of interest conflicts.

DISCLOSURES

The authors have nothing to disclose.

AUTHOR CONTRIBUTIONS

P.D.-B., C.P.-T., D.L., M.K., F.S., K.S., S.S., R.B.-D., E.N.O. and J.F. designed and analyzed experiments and prepared the manuscript. All authors read and approved the manuscript.

nuclear export. Mice lacking PKD1 in skeletal myocytes were resistant to Ang II-induced muscle wasting.

Conclusion—We propose that elevated Ang II serum concentrations, as occur in CHF patients, could activate the PKD1/HDAC5/TFEB/MuRF1 pathway to induce skeletal muscle wasting.

Keywords

TFEB; MuRF1; cardiac cachexia; skeletal muscle atrophy; Angiotensin II; transcription factor EB; histone deacetylase 5; protein kinase D1; congestive heart failure; gene expression/regulation; transcriptional regulation; skeletal myopathy exercise

INTRODUCTION

Skeletal muscle plasticity assures functional adaptation to physiological and pathological conditions by regulating muscle mass and fiber type.[1–3] Muscle mass is regulated by a well-controlled balance between protein synthesis and degradation and decreased.[4] Increased protein degradation and/or decreased protein synthesis result in skeletal muscle atrophy. Muscle disuse, neurological disorders, and aging belong to the best-studied conditions leading to atrophy. However, muscle atrophy and wasting also accompany diseases such as cancer[5] or end-stage congestive heart failure (CHF)[6], where cachexia is the major constituent.[6, 7] Although, the detailed mechanism of CHF-induced muscle atrophy is unknown angiotensin II (Ang II) has been implicated in this process. First, the renin-angiotensin-aldosterone system (RAAS) is activated and Ang II serum levels are increased in CHF patients.[8, 9] Second, reduced RAAS activity by angiotensin converting enzyme (ACE) inhibition reduced cachexia in CHF patients.[6] Third, Ang II leads to decreased muscle mass by increased ubiquitin-proteasome system (UPS)-dependent muscular protein degradation.[10] Ang II increases UPS-mediated protein degradation by inducing muscle RING-finger-1 (MuRF1) expression.[11–13] This muscle-enriched E3 ubiquitin ligase is a key mediator of muscle atrophy.[14] However, the Ang II-activated signaling pathway increasing *MuRF1* expression in muscle is not well understood. To search for novel transcription factors involved in Ang II-induced *MuRF1* expression, we performed a cDNA expression screen. The basic helix-loop-helix (bHLH) transcription factor EB (TFEB) was identified as potent *MuRF1* inducer. TFEB activity was regulated via the Ang II/protein kinase D1 (PKD1)/histone deacetylase-5 (HDAC5) signal transduction pathway. Inhibiting TFEB abolished Ang II-induced atrophy in vitro. We suggest that Ang II-induced skeletal muscle wasting could be mediated at least in part by the PKD1/HDAC5/TFEB/MuRF1 pathway.

METHODS

An expanded Materials and Methods section is included in the Online Supplement.

RESULTS

To discover novel regulators of *MuRF1* expression we performed a cDNA expression screen using a luciferase reporter controlled by the human *MuRF1*-promoter (−5,002 bp upstream of the transcription start site, Hs_*MuRF1*-Luc) and a human skeletal muscle cDNA library

according to our previous work.[15, 16] The screening procedure is described (Online Figure I). We expressed pools of clones from the cDNA expression library in COS-7 cells and quantified activation of Hs_*MuRF1*-Luc by luciferase assays. Following sib selection, a cDNA encoding the transcription factor EB (TFEB) was identified as strong inducer of Hs_*MuRF1*-Luc (Online Figure II). TFEB belongs to the MITF/TFE family of basic helix-loop-helix leucine zipper (bHLH-LZ) transcription factors. Recently, TFEB has been shown to regulate lysosomal biogenesis, autophagy and lipid metabolism.[17–20] However, regulation of *MuRF1* expression by TFEB has not been reported.

To confirm the results from the cDNA expression screen we generated cDNA expression constructs of TFEB and tested if overexpression of TFEB activates Hs_*MuRF1*-Luc activity. TFEB increased Hs_*MuRF1*-Luc activity in a dose dependent manner indicating that TFEB activates *MuRF1* expression (Figure 1A). Because MuRF1 is primarily contained in skeletal muscle and heart[14] whereas TFEB is ubiquitously expressed,[21, 22] quantitative real-time PCR (qRT-PCR) was used to test if *TFEB* was also expressed in striated muscle. To investigate whether *TFEB* is expressed in a fiber-type specific manner we quantitated its expression in muscle primarily containing fast twitch/type II fibers (*tibialis anterior*, *extensor digitorum longus*), and both fast twitch/type II and slow twitch/type-I fibers (*soleus*, *gastrocnemius/plantaris*). To compare muscular *TFEB* expression with expression in liver and spleen, both organs were included into the analysis. Our data showed that *TFEB* expression in skeletal muscle and the heart is similar with its expression in liver where the function is well described.[18] No evidence was found for fibre type related differences in *TFEB* expression. However, because TFEB was contained in all skeletal muscle and all parts of the heart analyzed, TFEB could contribute to transcriptional regulation of *MuRF1* in muscles (Figure 1B). To test if TFEB increases endogenous MuRF1 mRNA expression and protein content in myocytes, we used qRT-PCR and Western blot analysis of lysates from C2C12 myoblasts transfected with cDNA expression plasmids encoding TFEB. Overexpressed TFEB increased endogenous MuRF1 mRNA expression (Figure 1C) and protein content (Figure 1D) in these cells. In addition to MuRF1, we analyzed the effect of TFEB on *MuRF2* and *MuRF3* expression, homologous MuRF family members that are also restricted to striated muscles. In contrast to *MuRF1*, TFEB did not elevate *MuRF2* and *MuRF3* expression (Figure 1C). Loss-of-function experiments were performed to investigate if TFEB is required for basal *MuRF1* expression in C2C12 myoblasts. The siRNA mediated TFEB knockdown led to reduced MuRF1 mRNA expression and protein content in C2C12 myoblasts in vitro (Figure 1E and F).

To uncover cis-regulatory elements in the *MuRF1*-promoter mediating responsiveness to TFEB, we generated Hs_*MuRF1*-Luc deletion mutants. Deletion of nucleotides from position −5,002 bp down to −300 bp relative to the transcription start site of the *MuRF1*-promoter had no effect on TFEB induced Hs_*MuRF1*-Luc activity in HEK-293 cells (Figure 2A, Online Figure III). However, further size reduction of the *MuRF1*-promoter led to a decline in TFEB responsiveness. More specifically, *MuRF1*-promoter fragments shorter than 300 bp showed a decreased TFEB responsiveness (Figure 2A). These data implicated TFEB binding sites between 300 bp and the transcription start site of the *MuRF1*-promoter. We used the −543 bp *MuRF1*-promoter fragment for further analysis. Because TFEB is known

to bind to specific E-box motifs in the promoter of lysosomal genes, so called CLEAR elements[23, 24], the sequence of the −543 bp *MuRF1*, we analyzed the promoter fragment for conserved E-box motifs and found four (Figure 2B). E-box 1 (−41 to −46 bp), E-box 2 (−63 to −68 bp) and E-box 3 (−139 to −144 bp) showed a high degree of sequence conservation across species. Because E-box 4 (−299 to −304 bp) was less conserved, and not present in all species, we focused on E-box 1, 2 and 3 for further analyses (Figure 2B). To investigate the importance of E-box 1 to 3 for TFEB induced *MuRF1* expression, site-directed mutagenesis was used to mutate these E-box motifs from CANNTG to ATNNTG, known to inhibit E-box functionality,[23] in the −543 bp Hs_*MuRF1*-Luc construct (Figure 2B). Mutation of E-box 1 and 3 abolished TFEB induced *MuRF1* expression, whereas mutation of E-box 2 had only minor effects (Figure 2C). These data indicate that E-box 1 and 3 in the human *MuRF1*-promoter mediate TFEB induced *MuRF1* expression. We next used chromatin-immunoprecipitation followed by qRT-PCR (ChIP-PCR) to elucidate if TFEB binds to the conserved E-box motifs E-box 1, 2, and 3 in the endogenous *MuRF1*-promoter. ChIP-PCR experiments were performed using an anti-TFEB antibody to test if endogenous TFEB was bound to the endogenous MuRF1-promoter. These experiments confirmed direct binding of endogenous TFEB to E-box 1, 2, and 3 to the endogenous *MuRF1*-promoter (Figure 2D). In addition, we tested if overexpressed TFEB binds to the endogenous *MuRF1*-promoter. Chromatin of C2C12 myoblasts transfected with vector control, FLAG-TFEB or TFEB-Myc(His)$_6$, was immunoprecipitated with anti-FLAG and Ni^{2+}-NTA agarose, respectively. An enrichment of the *MuRF1*-promoter sequence surrounding E-box 1, 2, and 3 in the immunoprecipitated DNA from FLAG-TFEB and TFEB-Myc(His)$_6$, respectively, indicated binding of overexpressed TFEB to the endogenous *MuRF1*-promoter (Online Figure IVA, B). Because MuRF1 is known to mediate Ang II-induced skeletal muscle atrophy,[11–13] we tested if Ang II regulates TFEB binding to the *MuRF1*-promoter. ChIP-PCR assays were performed using chromatin from Ang II-treated C2C12 cells. This experiment showed that Ang II increased TFEB binding to E-box 1, 2, and 3 in the endogenous *MuRF1*-promoter (Figure 2E). Since starvation was shown to increase TFEB activity in other cell types,[23, 24] we tested if starvation increases binding of TFEB to the endogenous *MuRF1*-promoter. Indeed, starvation increased binding of endogenous TFEB to the endogenous *MuRF1*-promoter in C2C12 myoblasts (Figure 2F). In summary, our data show that TFEB constitutively binds to conserved E-box elements in the *MuRF1*-promoter in myocytes and that Ang II signaling, as well as starvation, increases the amount of TFEB bound to E-box 1, 2, and 3 in the *MuRF1*-promoter.

Although the function and regulation of TFEB in non-muscle cells is well described,[18–20, 25] its function in myocytes is not well understood. We next performed immunocytochemistry and immunofluorescence microscopy to investigate subcellular localization of TFEB in C2C12 myoblasts. We generated cDNA expression plasmids encoding wild-type or mutant TFEB (Figure 3A) and transfected them into C2C12 cells. Overexpressed wild-type TFEB was localized in the nucleus, cytosol and vesicular structures (Figure 3B, Figure 4B). Deletion of amino acids (AA) 1–127 (128-C), containing the glycine-rich (GR) domain, or AA129-237, containing regulatory serine residues in TFEB[20], had no effect on TFEBs subcellular localization (Figure 3B). In contrast, deletion of AA238-400, encoding the bHLH and leucine zipper (LZ) domain, and AA299-352, encoding only the bHLH domain,

abolished nuclear localization of TFEB in C2C12 myocytes (Figure 3B). These data indicate that the bHLH domain mediates nuclear localization of TFEB. Luciferase assays were used to test if these changes in subcellular localization also affected the ability of TFEB to increase *MuRF1* expression. As expected TFEB deletion mutants AA299-352 and AA238-400, which were not found in the nucleus, failed to increase *MuRF1* expression (Figure 3C). In contrast, TFEB deletion mutants AA128-C and AA129-237 increased *MuRF1* expression but not to the same extend as wild-type TFEB (Figure 3C). We used western blot analysis to test if deletion mutant TFEB AA299-352 would also fail to increase the endogenous MuRF1 protein content in C2C12 cells. No increase in endogenous MuRF1 protein content was detected after transfection of this deletion mutant (Figure 3D). These data indicate that in myocytes TFEB is localized to the cytoplasm and to the nucleus, and that its nuclear localization is important for its effects on *MuRF1* expression.

Recently, we reported that the bHLH transcription factor myogenin increases *MuRF1* expression and that class II histone deacetylases (HDACs) inhibit the activity of myogenin at the *MuRF1*-promoter.[26] Because TFEB was localized to both the nucleus and the cytoplasm of myocytes, we hypothesized that class IIa HDACs inhibit the activity of nuclear TFEB. According to our working hypothesis we focused on HDAC5, because Ang II was shown to repress HDAC5 activity in smooth muscle cells via regulation of its nuclear-to-cytoplasmic export.[27] Using luciferase assays, we found that HDAC5 inhibited TFEB induced *MuRF1* expression (Figure 4A). To elucidate the nature of this inhibitory effect, we performed immunocytochemistry and coimmunoprecipitation experiments to test if TFEB and HDAC5 colocalized and physically interacted with each other, respectively. As shown by immunocytochemistry staining, TFEB and HDAC5 colocalized in the nucleus and in cytosolic vesicular structures when coexpressed in C2C12 myoblasts (Figure 4B). Coimmunoprecipitation experiments showed that TFEB and HDAC5 physically interacted with each other (Figure 4C). Further coimmunoprecipitation experiments were performed to map the interacting region in TFEB and HDAC5 using expression plasmids encoding wild-type and deletion mutants of TFEB and HDAC5 (Figure 4D, 4E). Deletion of amino acids 1–127 of TFEB (TFEB 128-C) abolished interaction with wild-type HDAC5. Deletion of AA129-237 in TFEB resulted in decreased binding between TFEB and HDAC5. Removal of the bHLH domain (TFEB Δ299–352) or the bHLH-LZ domain in TFEB (TFEB Δ238–400) had no effect on interaction between TFEB and HDAC5 (Figure 4D). These data indicate that direct interaction between TFEB and HDAC5 is mediated by AA1-237 at the amino-terminus of TFEB. Moreover, using truncated variants of HDAC5 in coimmunoprecipitation experiments followed by Western blotting we found that the HDAC5 deletion mutants AA100-C and AA175-C failed to interact with wild-type TFEB (Figure 4E). Luciferase assays were performed to elucidate if interaction between TFEB and HDAC5 is required for the repressive effect of HDAC5 on TFEB activity. As anticipated, activity of those TFEB mutants that did not interact with HDAC5 were not repressed (Figure 4F). Likewise, HDAC5 deletion mutants AA100-C and AA175-C that did not interact with TFEB, or AA1–664 that lacks the deacetylase domain of HDAC5, did not repress TFEB-induced *MuRF1* expression. Whereas, the HDAC5 deletion mutant AA51-C that still interacts with TFEB, inhibited TFEB-induced *MuRF1* expression to similar extend as wild-type HDAC5 (Figure

4G). These data indicate that direct interaction between TFEB and HDAC5 is required for HDAC5 mediated inhibition of TFEB.

PKD1 inhibits HDAC5 mediated repression of TFEB

We previously reported that the stress responsive serine/threonine kinase protein kinase D1 (PKD1) plays a regulatory role in muscle remodeling via phosphorylation and nuclear export of HDAC5.[28, 29] Therefore, we reasoned that PKD1 might play a role in regulation of the HDAC5/TFEB/MuRF1 axis. PKD1 phosphorylates HDAC5 enabling binding of 14-3-3 chaperon proteins and mediating its nuclear export in a CRM1-dependent manner.[29] Phosphoserines 259 and 498 in HDAC5 serve as binding sites for the chaperone protein 14-3-3.[30] To confirm if binding between PKD1 and HDAC5 leads to PKD1-mediated phosphorylation of the 14-3-3 consensus sites in HDAC5, we performed a UAS-luciferase assay as published recently.[16] In this assay, the N-terminus of HDAC5 is fused to the GAL4 DNA-binding domain, and 14-3-3 is fused to the VP16 transactivation domain. Under normal growth conditions, HDAC5 is not phosphorylated in COS-7 cells. Thus, GAL4-HDAC5 cannot interact with 14-3-3-VP16 and the GAL4-dependent luciferase reporter (UAS-luciferase) cannot be activated. Expression plasmids encoding these fusion proteins, together with UAS-luciferase, were transfected into COS-7 cells together with wild-type, constitutive-active (CA), or inactive (kinase-dead) PKD1 and increasing amounts of PKD1 CA expression plasmids, respectively. Wild-type PKD1 and constitutive-active PKD1 increased UAS-luciferase activity (Figure 5A). This activation was dependent upon the amount of PKD1 transfected (Figure 5B). These data indicate that PKD1 creates phospho-14-3-3 recognition motifs in HDAC5, which recruit 14-3-3 chaperone proteins eventually leading to its nuclear export. Coimmunoprecipitation experiments showed that wild-type PKD1 interacted avidly with wild-type HDAC5 (Figure 5C). Further mapping experiments showed that AA360-601 in HDAC5 were responsible for interaction between HDAC5 and PKD1 (Figure 5D, Online Figure V). In addition, we identified the cysteine-rich region 1a (C1a) in PKD1 to be responsible for the interaction between PKD1 and HDAC5 (Figure 5E, F). We hypothesized that PKD1 inhibits HDAC5-mediated repression of TFEB-induced *MuRF1* expression by facilitating nuclear export of HDAC5. Immunocytochemistry showed that colocalization of TFEB and HDAC5 in the nucleus was abolished when PKD1 was coexpressed in C2C12 myoblasts (Figure 5G), indicating that PKD1 controls TFEB activity via regulation of its physical interaction with its repressor HDAC5. Luciferase assays were performed to elucidate if PKD1 inhibits HDAC5-mediated repression of TFEB induced *MuRF1* expression. Expression plasmids encoding HDAC5, TFEB, and *MuRF1*-Luc were transfected together with PKD1 in COS-7 cells and their effect on *MuRF1*-promoter activity was investigated. Indeed, PKD1 abolished HDAC5-mediated inhibition of TFEB induced *MuRF1* expression (Figure 5H).

Ang II-induced atrophy is attenuated by knockdown of TFEB in C2C12 myotubes

Because Ang II activates PKD1 activity[27] and induces muscle atrophy by increasing *MuRF1* expression,[11–13] we reasoned that TFEB mediates Ang II-induced *MuRF1* expression. To test this hypothesis, we used siRNA targeting *TFEB* in C2C12 myotubes and treated these cells either with Ang II or vehicle for 24 hours. C2C12 myotubes transfected with scrambled siRNA and treated with Ang II or vehicle for 24 hours served as control. A qRT-PCR

showed that knockdown of TFEB decreased Ang II-induced *MuRF1* mRNA expression (Figure 6A). To test whether Ang II-induced *MuRF1* expression was mediated by HDAC5, we transfected a signal-resistant FLAG-HDAC5 S259/498A, harboring alanines in place of serines 259 and 498, which are required for nuclear export of HDAC5, into C2C12 myoblasts for 24 hours and treated these cells either with Ang II or vehicle for 24 hours. C2C12 myoblasts transfected with vector control and treated with Ang II or vehicle for 24 hours served as control. qRT-PCR showed that overexpression of signal-resistant HDAC5 reduced Ang II-induced *MuRF1* mRNA expression (Figure 6B). Additionally, we tested whether or not TFEB mediates Ang II-induced myofiber atrophy. To test this hypothesis, we used siRNA targeting *TFEB* in differentiated C2C12 myotubes and treated these cells either with Ang II or vehicle for 48 hours. C2C12 myotubes transfected with scrambled siRNA and treated with Ang II or vehicle for 48 hours served as control. Myotube diameters were measured using ImageJ software. As expected, Ang II treatment induced atrophy of C2C12 myotubes. Knockdown of TFEB significantly reduced Ang II-induced atrophy of C2C12 myotubes (Figure 6C, D). These results indicate that TFEB mediates Ang II-induced *MuRF1* expression and myocyte atrophy.

PKD1 ablation in skeletal myocytes attenuates Ang II-induced muscular atrophy in vivo

Given that Ang II is a strong activator of the PKD1/HDAC5/TFEB/MuRF1 axis, we hypothesized that absence of *PKD1* inhibits Ang II-induced muscle atrophy in vivo. We generated mice with a skeletal muscle specific deletion of *PKD1* (*PKD1*$^{\text{loxP/loxP; MCK-CRE}}$; conditional *PKD1* knockout, *PKD1* cKO) to investigate the importance of muscular *PKD1* for Ang II-mediated muscle *atrophy* in vivo as recently described.[28, 31] *PKD1*$^{\text{WT/WT; MCK-CRE}}$ mice were used to control for unspecific MCK-CRE-mediated effects on the skeletal muscle. *PKD1* cKO mice and *PKD1*$^{\text{WT/WT; MCK-CRE}}$ controls were treated with chronic infusion of Ang II (1.5 μg/KG/min)[12, 13, 32] via osmotic minipumps for 24 hours and seven days. Ang II treatment led to a significant decrease in *gastrocnemius/plantaris* weight in *PKD1*$^{\text{WT/WT; MCK-CRE}}$ mice, but not *PKD1* cKO mice after seven days' treatment (Figure 7A). Accordingly, myocytes-cross-sectional area (MCSA) was reduced in Ang II treated *PKD1*$^{\text{WT/WT; MCK-CRE}}$ mice, but not in *PKD1* cKO mice animals after seven days' Ang II treatment (Figure 7B). ChIP-PCR assays were performed using chromatin from *gastrocnemius/plantaris* of 24 hours Ang II- and vehicle-treated *PKD1*$^{\text{WT/WT; MCK-CRE}}$ and cKO mice. This experiment showed that Ang II increased TFEB binding to E-box 1 on the endogenous *MuRF1*-promoter of *PKD1*$^{\text{WT/WT; MCK-CRE}}$, but not cKO mice (Figure 7C). A qRT-PCR and Western blot analysis showed that 24 hours Ang II treatment increased MuRF1 mRNA and protein expression in *gastrocnemius/plantaris* of *PKD1*$^{\text{WT/WT; MCK-CRE}}$ mice, but not *PKD1* cKO mice (Figure 7D, E). In contrast, MuRF1 mRNA and protein expression remained unchanged after seven days' Ang II treatment (Figure 7D, E). These data show that Ang II-induced muscular atrophy is at least partially regulated via PKD1-dependent regulation of TFEB-mediated *MuRF1* expression.

DISCUSSION

We identified TFEB as a novel transcriptional regulator of *MuRF1*. Our study shows that nuclear TFEB specifically binds to conserved E-box motifs in the *MuRF1*-promoter

localized close to its transcription start site. In myocytes, binding of TFEB to the *MuRF1*-promoter was increased by Ang II treatment and by starvation in vitro. We demonstrated that PKD1, together with HDAC5, controls TFEB activity at the *MuRF1*-promoter. Our data imply that the PKD1/HDAC5/TFEB/MuRF1 axis mediates Ang II-induced skeletal muscle atrophy (Figure 8). Inhibition of this signaling pathway could be important in combating Ang II-associated muscle wasting disorders, such as CHF-induced cachexia.

We searched for novel regulators of *MuRF1* expression. To this end, we used a cDNA library generated from human skeletal muscle and skeletal muscle cells to perform a mechanistic analysis. This approach differs from prior studies investigating the function of TFEB, which have primarily been performed in HeLa cells and in liver.[23, 24] These studies showed that TFEB is ubiquitously expressed.[33] However, expression of TFEB in the skeletal muscle and the heart and transcriptional regulation of the muscle enriched E3 ubiquitin ligase MuRF1 clearly argue for its functional importance in muscle cells. TFEB was reported to promote expression of genes involved in early and late lysosomal biogenesis by direct binding to specific E-box motifs at their promoters.[23, 24] TFEB also regulates biogenesis of autophagosomes, the fusion of autophagosomes with lysosomes, and autophagic flux.[18] Based on its function in lysosomal biogenesis, the gene network regulated by TFEB was named CLEAR (*Coordinated Lysosomal Expression and Regulation*) and the specific E-box motifs TFEB binds to CLEAR elements. The consensus sequence of the CLEAR element was resolved as CACGTG,[23, 24] which is consistent with a specific E-box motif (CANNTG). The sequence of the conserved E-box motifs in the *MuRF1*-promoter to which TFEB binds clearly differs from the described CLEAR element consensus sequence. E-boxes 1 and 3, predominantly mediating TFEB-induced *MuRF1* expression in myocytes, share the consensus site CATGTG, which was highly conserved throughout species. Nevertheless, since TFEB strongly increased *MuRF1* expression via these E-box motifs and the fact that increased binding of TFEB to the *MuRF1* promoter was found after Ang II treatment and starvation supports the idea that these E-box motifs are functional. The distinct differences in the sequence between the E-box motifs in the *MuRF1* promoter and CLEAR elements imply that TFEB also regulates the expression of genes not involved in lysosomal or autophagosomal biogenesis. Although we would like to speculate that the PKD1/HDAC5/TFEB axis also regulates lysosomal and autophagosomal protein degradation in muscle, such experiments were beyond the scope of this work. We contribute the findings that TFEB additionally regulates expression of *MuRF1*, a muscle enriched E3 ubiquitin ligase, which plays a key role in UPS dependent protein degradation in muscle atrophy.[14] Therefore, we believe that TFEB serves as a nodal transcription factor regulating not only lysosomal and autophagosomal, but also UPS dependent protein degradation in muscle cells.

Recent data suggest that only the subset of TFEB binding sites associated with proximal promoter regions in lysosomal genes is functional. Most TFEB binding sites were localized in close proximity to the transcription start sites, with most sites lying between positions −300 bp to +100 bp of the 5’ end of genes. Genes highly responsive to TFEB often display clustered TFEB binding sites.[24] We found E-box 1, 2, and 3 in the *MuRF1* promoter, the sites at which TFEB binds, are located close to the transcription start site of *MuRF1*.

Importantly, these E-box motifs were also clustered. In contrast, E-box 4 that is located further upstream of the transcription start site of *MuRF1* and that is not conserved throughout species, was not involved in TFEB-mediated *MuRF1* expression. In summary, our data indicate that TFEB increases *MuRF1* expression via conserved and clustered E-box elements located within the proximal promoter region of *MuRF1*.

Previous studies showed that TFEB is predominantly localized in the cytoplasm of HEK-293T cells and that its phosphorylation status and cytosolic-to-nuclear shuttling regulate TFEB activity.[20] The kinases mTORC1 and ERK were shown to be important in that regard.[20, 34, 35] In the presence of nutrients, mTORC1 phosphorylates TFEB thereby facilitating its binding to 14-3-3 proteins and mediating its retention in the cytoplasm. Conversely, reduced mTORC1 activity increases TFEB shuttling into the nucleus.[20, 34, 35] Whether or not mTORC1 and ERK regulate TFEB activity in myocytes is unknown. However, we report that TFEB is localized to the cytoplasm and the nucleus of myocytes. Our data are supported by others showing that 20 to 30% of TFEB is contained in the nucleus of several cell lines, such as patient-derived fibroblasts,[36] HeLa cells,[18] ARPE-19 cells,[34] and mouse embryonic fibroblasts.[23] Our observation that TFEB knockdown reduced baseline *MuRF1* expression in C2C12 cells indicates that TFEB plays a role in regulation of baseline gene expression and supports the notion that nuclear TFEB is functionally active. We also describe the fact that nuclear TFEB was bound to the *MuRF1* promoter already at baseline and that this binding was increased by Ang II treatment or starvation. TFEB mutants that do not bind to E-box motifs are unable to translocate to the nucleus did not increase *MuRF1* expression. Importantly, when localized in the nucleus TFEB associated with HDAC5. HDAC5, which is primarily localized to the nucleus,[29] directly interacted with TFEB in the nucleus and inhibited its activity. HDAC5-deletion mutants not interacting with *TFEB* did not repress TFEB-induced *MuRF1* expression. Our data indicate that the activity of TFEB is regulated at least at two levels, first by regulation of the subcellular localization of TFEB and second by repression of its activity by HDAC5 once it is localized to the nucleus.

Recently we reported that myogenin, another HLH transcription factor, is involved in neurogenic atrophy and that its activity is regulated by HDAC4 and HDAC5.[26] Our data implicated additional targets of these HDACs promoting neurogenic atrophy. We also showed that myogenin was necessary, but not sufficient, to regulate the genetic program for muscle atrophy and proposed additional important signals for this process. We report that TFEB could at least partially account for these differences. We define TFEB as additional target of HDAC5 and describe that TFEB`s activity is regulated via its interaction with HDAC5. However, the importance of this pathway in neurogenic atrophy is unknown.

MuRF1 is a key enzyme in UPS dependent skeletal muscle atrophy and mediates UPS dependent degradation of myofibrillar proteins,[37–40] such as myosin heavy chain and troponin I.[41–43] MuRF1 expression and protein content are increased in various animal models of muscle atrophy,[14, 44] and germ-line *MuRF1* deletion prevents muscle atrophy in mice.[14] MuRF1 is also increased in skeletal muscle of CHF patients with wasting.[45] Importantly, *MuRF1* expression was increased in Ang II-induced muscle atrophy indicating that Ang II increases muscle protein breakdown via *MuRF1*.[11–13] However, the signaling

pathway mediating Ang II-induced *MuRF1* expression in muscle was unknown. Recently, investigators reported that Ang II regulates *MuRF1* expression in an Akt-Foxo-independent pathway,[12] leaving the question regarding the role of Ang II-induced *MuRF1* expression still open. We show that Ang II induces skeletal muscle atrophy by activation of TFEB. This process involves HDAC5-mediated repression of TFEB induced *MuRF1* expression and negative regulation of HDAC5 by PKD1. We hypothesize that Ang II induces *MuRF1* expression via the PKD1/HDAC5/TFEB axis. Based on our data we speculate that elevated Ang II serum concentrations, as occur in CHF patients, could activate this pathway.[8] Because cardiac cachexia is a life threatening complication, therapeutic interventions counteracting muscle atrophy and its accompanying weakness could be useful to prevent immobilization and increase quality of life. However, further studies are needed to elucidate the importance of this pathway in vivo.

We speculate that the Ang II/PKD1/HDAC5/TFEB/MuRF1 pathway described here is involved in skeletal muscle wasting of CHF patients. However, we have not proved such an association. To test if this pathway is involved in skeletal muscle atrophy caused by CHF the atrophic response of *PKD1* KO mice subjected to standard heart-failure models, such as coronary ligation to induce myocardial infarction[46], transverse aortic constriction[47], genetic heart failure models such as deletion of the muscle limb protein,[48] and toxic doxorubicine-induced cardiomyopathy[49,50, 51] could be investigated. However, CHF is a complex syndrome that in addition to the RAAS, involves many different neuroendocrine pathways, such as the sympathetic nervous system, the endothelin system, and inflammatory mediators.[51–55] In addition, CHF leads to immobility, which also causes muscle atrophy. All these factors add to the complexity of the aforementioned experiment. We specifically focused on Ang II-mediated muscle atrophy and investigated its downstream signal transduction pathway. Ang II serum levels are increased in heart failure[9, 56–60] and its role in muscle wasting is well established[12, 13, 32]. However, our model spans only one week and we did not show heart failure in our model. Further studies are needed to elucidate whether or not the PKD1/HDAC5/TFEB/MuRF1 axis can also be utilized and activated by other signaling pathways involved in CHF-associated muscle wasting. Finally, the amount of Ang II infused into mice to induced muscle atrophy in this study surely resulted in higher Ang II plasma levels than those observed in patients with CHF. We used this Ang II dose because it induces atrogene gene expression after 24 hours and muscle atrophy after seven days.[12, 13, 32] We cannot directly compare Ang II plasma levels between patients and our contrived mouse model. Nonetheless, our data show that deletion of *PKD1* prevents Ang II-induced muscle atrophy, when Ang II was infused at a rate of 1.5 μg/kg/min.

Supplementary Material

Refer to Web version on PubMed Central for supplementary material.

ACKNOWLEDGEMENT

We thank Friedrich C. Luft for helpful advice on the manuscript. We thank Janine Woehlecke, Anika Lindner, Josephine Russ and Marcel Mehl for excellent technical assistance.

SOURCES OF FUNDING

The Deutsche Forschungsgemeinschaft (FI 965/2-1, FI 965/4-1), Muscular Dystrophy Association (MDA4013), Marie Curie International Reintegration grant (FP7-PEOPLE-IRG-2008 - 231014), the Experimental and Clinical Research Center (ECRC), and the Deutsche Gesellschaft für Muskelkranke e.V. all supported this work. This work was also supported by grants from the NIH (HL-077439, HL-111665, HL-093039, DK-099653 and U01-HL-100401), Fondation Leducq Networks of Excellence, Cancer Prevention and Research Institute of Texas and the Robert A. Welch Foundation (grant 1-0025 to E.N.O.).

Nonstandard Abbreviations and Acronyms

ACE	angiotensin converting enzyme
Ang II	angiotensin II
bHLH-LZ	basic helix-loop-helix leucine zipper
CHF	congestive heart failure
ChiP	chromatin immunoprecipitation
CLEAR	coordinated lysosomal expression and regulation
GAPDH	glyceraldehyde 3-phosphate dehydrogenase
HDAC5	histone deacetylase 5
HRP	horseradish peroxidase
Luc	luciferase
MuRF	muscle RING-finger
PKD1	protein kinase D1
qRT-PCR	quantitative real-time PCR
RAAS	renin-angiotensin aldosterone system
siRNA	small interfering RNA
TFEB	transcription factor EB
UPS	ubiquitin proteasome system

REFERENCES

1. Ciciliot S, Rossi AC, Dyar KA, Blaauw B, Schiaffino S. Muscle type and fiber type specificity in muscle wasting. Int J Biochem Cell Biol. 2013; 45:2191–2199. [PubMed: 23702032]
2. Borina E, Pellegrino MA, D'Antona G, Bottinelli R. Myosin and actin content of human skeletal muscle fibers following 35 days bed rest. Scandinavian journal of medicine & science in sports. 2010; 20:65–73. [PubMed: 19883388]
3. Snow LM, Sanchez OA, McLoon LK, Serfass RC, Thompson LV. Effect of endurance exercise on myosin heavy chain isoform expression in diabetic rats with peripheral neuropathy. American journal of physical medicine & rehabilitation / Association of Academic Physiatrists. 2005; 84:770–779. [PubMed: 16205433]
4. Ciechanover A. The ubiquitin proteolytic system: From a vague idea, through basic mechanisms, and onto human diseases and drug targeting. Neurology. 2006; 66:S7–S19. [PubMed: 16432150]
5. Vaughan VC, Martin P, Lewandowski PA. Cancer cachexia: Impact, mechanisms and emerging treatments. J Cachexia Sarcopenia Muscle. 2013; 4:95–109. [PubMed: 23097000]

6. Anker SD, Ponikowski P, Varney S, Chua TP, Clark AL, Webb-Peploe KM, Harrington D, Kox WJ, Poole-Wilson PA, Coats AJ. Wasting as independent risk factor for mortality in chronic heart failure. Lancet. 1997; 349:1050–1053. [PubMed: 9107242]
7. Anker MS, von Haehling S, Springer J, Banach M, Anker SD. Highlights of mechanistic and therapeutic cachexia and sarcopenia research 2010 to 2012 and their relevance for cardiology. Archives of medical science : AMS. 2013; 9:166–171. [PubMed: 23515589]
8. Anker SD, Negassa A, Coats AJ, Afzal R, Poole-Wilson PA, Cohn JN, Yusuf S. Prognostic importance of weight loss in chronic heart failure and the effect of treatment with angiotensin-converting-enzyme inhibitors: An observational study. Lancet. 2003; 361:1077–1083. [PubMed: 12672310]
9. Roig E, Perez-Villa F, Morales M, Jimenez W, Orus J, Heras M, Sanz G. Clinical implications of increased plasma angiotensin ii despite ace inhibitor therapy in patients with congestive heart failure. European heart journal. 2000; 21:53–57. [PubMed: 10610744]
10. Brink M, Price SR, Chrast J, Bailey JL, Anwar A, Mitch WE, Delafontaine P. Angiotensin ii induces skeletal muscle wasting through enhanced protein degradation and down-regulates autocrine insulin-like growth factor i. Endocrinology. 2001; 142:1489–1496. [PubMed: 11250929]
11. Song YH, Li Y, Du J, Mitch WE, Rosenthal N, Delafontaine P. Muscle-specific expression of igf-1 blocks angiotensin ii-induced skeletal muscle wasting. J Clin Invest. 2005; 115:451–458. [PubMed: 15650772]
12. Yoshida T, Semprun-Prieto L, Sukhanov S, Delafontaine P. Igf-1 prevents ang ii-induced skeletal muscle atrophy via akt- and foxo-dependent inhibition of the ubiquitin ligase atrogin-1 expression. American journal of physiology. Heart and circulatory physiology. 2010; 298:H1565–H1570. [PubMed: 20228261]
13. Semprun-Prieto LC, Sukhanov S, Yoshida T, Rezk BM, Gonzalez-Villalobos RA, Vaughn C, Michael Tabony A, Delafontaine P. Angiotensin ii induced catabolic effect and muscle atrophy are redox dependent. Biochem Biophys Res Commun. 2011; 409:217–221. [PubMed: 21570954]
14. Bodine SC, Latres E, Baumhueter S, Lai VK, Nunez L, Clarke BA, Poueymirou WT, Panaro FJ, Na E, Dharmarajan K, Pan ZQ, Valenzuela DM, DeChiara TM, Stitt TN, Yancopoulos GD, Glass DJ. Identification of ubiquitin ligases required for skeletal muscle atrophy. Science. 2001; 294:1704–1708. [PubMed: 11679633]
15. Song K, Backs J, McAnally J, Qi X, Gerard RD, Richardson JA, Hill JA, Bassel-Duby R, Olson EN. The transcriptional coactivator camta2 stimulates cardiac growth by opposing class ii histone deacetylases. Cell. 2006; 125:453–466. [PubMed: 16678093]
16. Chang S, Bezprozvannaya S, Li S, Olson EN. An expression screen reveals modulators of class ii histone deacetylase phosphorylation. Proc Natl Acad Sci U S A. 2005; 102:8120–8125. [PubMed: 15923258]
17. Sardiello M, Ballabio A. Lysosomal enhancement: A clear answer to cellular degradative needs. Cell Cycle. 2009; 8:4021–4022. [PubMed: 19949301]
18. Settembre C, Di Malta C, Polito VA, Garcia Arencibia M, Vetrini F, Erdin S, Erdin SU, Huynh T, Medina D, Colella P, Sardiello M, Rubinsztein DC, Ballabio A. Tfeb links autophagy to lysosomal biogenesis. Science. 2011; 332:1429–1433. [PubMed: 21617040]
19. Settembre C, De Cegli R, Mansueto G, Saha PK, Vetrini F, Visvikis O, Huynh T, Carissimo A, Palmer D, Klisch TJ, Wollenberg AC, Di Bernardo D, Chan L, Irazoqui JE, Ballabio A. Tfeb controls cellular lipid metabolism through a starvation-induced autoregulatory loop. Nat Cell Biol. 2013; 15:647–658. [PubMed: 23604321]
20. Settembre C, Zoncu R, Medina DL, Vetrini F, Erdin S, Huynh T, Ferron M, Karsenty G, Vellard MC, Facchinetti V, Sabatini DM, Ballabio A. A lysosome-to-nucleus signalling mechanism senses and regulates the lysosome via mtor and tfeb. EMBO J. 2012; 31:1095–1108. [PubMed: 22343943]
21. Fisher DE, Carr CS, Parent LA, Sharp PA. Tfeb has DNA-binding and oligomerization properties of a unique helix-loop-helix/leucine-zipper family. Genes Dev. 1991; 5:2342–2352. [PubMed: 1748288]
22. Kuiper RP, Schepens M, Thijssen J, van Asseldonk M, van den Berg E, Bridge J, Schuuring E, Schoenmakers EF, van Kessel AG. Upregulation of the transcription factor tfeb in t(6;11)

(p21;q13)-positive renal cell carcinomas due to promoter substitution. Hum Mol Genet. 2003; 12:1661–1669. [PubMed: 12837690]

23. Sardiello M, Palmieri M, di Ronza A, Medina DL, Valenza M, Gennarino VA, Di Malta C, Donaudy F, Embrione V, Polishchuk RS, Banfi S, Parenti G, Cattaneo E, Ballabio A. A gene network regulating lysosomal biogenesis and function. Science. 2009; 325:473–477. [PubMed: 19556463]
24. Palmieri M, Impey S, Kang H, di Ronza A, Pelz C, Sardiello M, Ballabio A. Characterization of the clear network reveals an integrated control of cellular clearance pathways. Hum Mol Genet. 2011; 20:3852–3866. [PubMed: 21752829]
25. Settembre C, Ballabio A. Tfeb regulates autophagy: An integrated coordination of cellular degradation and recycling processes. Autophagy. 2011; 7:1379–1381. [PubMed: 21785263]
26. Moresi V, Williams AH, Meadows E, Flynn JM, Potthoff MJ, McAnally J, Shelton JM, Backs J, Klein WH, Richardson JA, Bassel-Duby R, Olson EN. Myogenin and class ii hdacs control neurogenic muscle atrophy by inducing e3 ubiquitin ligases. Cell. 143:35–45. [PubMed: 20887891]
27. Xu X, Ha CH, Wong C, Wang W, Hausser A, Pfizenmaier K, Olson EN, McKinsey TA, Jin ZG. Angiotensin ii stimulates protein kinase d-dependent histone deacetylase 5 phosphorylation and nuclear export leading to vascular smooth muscle cell hypertrophy. Arterioscler Thromb Vasc Biol. 2007; 27:2355–2362. [PubMed: 17823368]
28. Kim MS, Fielitz J, McAnally J, Shelton JM, Lemon DD, McKinsey TA, Richardson JA, Bassel-Duby R, Olson EN. Protein kinase d1 stimulates mef2 activity in skeletal muscle and enhances muscle performance. Mol Cell Biol. 2008
29. Vega RB, Harrison BC, Meadows E, Roberts CR, Papst PJ, Olson EN, McKinsey TA. Protein kinases c and d mediate agonist-dependent cardiac hypertrophy through nuclear export of histone deacetylase 5. Mol Cell Biol. 2004; 24:8374–8385. [PubMed: 15367659]
30. Zhang CL, McKinsey TA, Chang S, Antos CL, Hill JA, Olson EN. Class ii histone deacetylases act as signal-responsive repressors of cardiac hypertrophy. Cell. 2002; 110:479–488. [PubMed: 12202037]
31. Fielitz J, Kim MS, Shelton JM, Qi X, Hill JA, Richardson JA, Bassel-Duby R, Olson EN. Requirement of protein kinase d1 for pathological cardiac remodeling. Proc Natl Acad Sci U S A. 2008; 105:3059–3063. [PubMed: 18287012]
32. Rezk BM, Yoshida T, Semprun-Prieto L, Higashi Y, Sukhanov S, Delafontaine P. Angiotensin ii infusion induces marked diaphragmatic skeletal muscle atrophy. PLoS One. 2012; 7:e30276. [PubMed: 22276172]
33. Kuiper RP, Schepens M, Thijssen J, Schoenmakers EF, van Kessel AG. Regulation of the mitf/tfe bhlh-lz transcription factors through restricted spatial expression and alternative splicing of functional domains. Nucleic Acids Res. 2004; 32:2315–2322. [PubMed: 15118077]
34. Martina JA, Chen Y, Gucek M, Puertollano R. Mtorc1 functions as a transcriptional regulator of autophagy by preventing nuclear transport of tfeb. Autophagy. 2012; 8:903–914. [PubMed: 22576015]
35. Roczniak-Ferguson A, Petit CS, Froehlich F, Qian S, Ky J, Angarola B, Walther TC, Ferguson SM. The transcription factor tfeb links mtorc1 signaling to transcriptional control of lysosome homeostasis. Sci Signal. 2012; 5:ra42. [PubMed: 22692423]
36. Song W, Wang F, Savini M, Ake A, di Ronza A, Sardiello M, Segatori L. Tfeb regulates lysosomal proteostasis. Hum Mol Genet. 2013; 22:1994–2009. [PubMed: 23393155]
37. Centner T, Yano J, Kimura E, McElhinny AS, Pelin K, Witt CC, Bang ML, Trombitas K, Granzier H, Gregorio CC, Sorimachi H, Labeit S. Identification of muscle specific ring finger proteins as potential regulators of the titin kinase domain. J Mol Biol. 2001; 306:717–726. [PubMed: 11243782]
38. Hirner S, Krohne C, Schuster A, Hoffmann S, Witt S, Erber R, Sticht C, Gasch A, Labeit S, Labeit D. Murf1-dependent regulation of systemic carbohydrate metabolism as revealed from transgenic mouse studies. J Mol Biol. 2008; 379:666–677. [PubMed: 18468620]
39. Witt CC, Witt SH, Lerche S, Labeit D, Back W, Labeit S. Cooperative control of striated muscle mass and metabolism by murf1 and murf2. Embo J. 2008; 27:350–360. [PubMed: 18157088]

40. Cohen S, Brault JJ, Gygi SP, Glass DJ, Valenzuela DM, Gartner C, Latres E, Goldberg AL. During muscle atrophy, thick, but not thin, filament components are degraded by murf1-dependent ubiquitylation. J Cell Biol. 2009; 185:1083–1095. [PubMed: 19506036]
41. Fielitz J, Kim MS, Shelton JM, Latif S, Spencer JA, Glass DJ, Richardson JA, Bassel-Duby R, Olson EN. Myosin accumulation and striated muscle myopathy result from the loss of muscle ring finger 1 and 3. J Clin Invest. 2007; 117:2486–2495. [PubMed: 17786241]
42. Clarke BA, Drujan D, Willis MS, Murphy LO, Corpina RA, Burova E, Rakhilin SV, Stitt TN, Patterson C, Latres E, Glass DJ. The e3 ligase murf1 degrades myosin heavy chain protein in dexamethasone-treated skeletal muscle. Cell Metab. 2007; 6:376–385. [PubMed: 17983583]
43. Kedar V, McDonough H, Arya R, Li HH, Rockman HA, Patterson C. Muscle-specific ring finger 1 is a bona fide ubiquitin ligase that degrades cardiac troponin i. Proc Natl Acad Sci U S A. 2004; 101:18135–18140. [PubMed: 15601779]
44. Glass DJ. Skeletal muscle hypertrophy and atrophy signaling pathways. Int J Biochem Cell Biol. 2005; 37:1974–1984. [PubMed: 16087388]
45. Gielen S, Sandri M, Kozarez I, Kratzsch J, Teupser D, Thiery J, Erbs S, Mangner N, Lenk K, Hambrecht R, Schuler G, Adams V. Exercise training attenuates MuRF-1 expression in the skeletal muscle of patients with chronic heart failure independent of age: the randomized Leipzig Exercise Intervention in Chronic Heart Failure and Aging catabolism study. Circulation. 2012 Jun 5; 125(22):2716–2727. [PubMed: 22565934]
46. Zolotareva AG, Kogan ME. Production of experimental occlusive myocardial infarction in mice. Cor et vasa. 1978; 20:308–314. [PubMed: 729388]
47. Rockman HA, Ross RS, Harris AN, Knowlton KU, Steinhelper ME, Field LJ, Ross J Jr, Chien KR. Segregation of atrial-specific and inducible expression of an atrial natriuretic factor transgene in an in vivo murine model of cardiac hypertrophy. Proc Natl Acad Sci U S A. 1991; 88:8277–8281. [PubMed: 1832775]
48. Arber S, Hunter JJ, Ross J Jr, Hongo M, Sansig G, Borg J, Perriard JC, Chien KR, Caroni P. Mlp-deficient mice exhibit a disruption of cardiac cytoarchitectural organization, dilated cardiomyopathy, and heart failure. Cell. 1997; 88:393–403. [PubMed: 9039266]
49. van der Vijgh WJ, van Velzen D, van der Poort JS, Schluper HM, Mross K, Feijen J, Pinedo HM. Morphometric study of myocardial changes during doxorubicin-induced cardiomyopathy in mice. European journal of cancer & clinical oncology. 1988; 24:1603–1608. [PubMed: 3208804]
50. Houser SR, Margulies KB, Murphy AM, Spinale FG, Francis GS, Prabhu SD, Rockman HA, Kass DA, Molkentin JD, Sussman MA, Koch WJ. American Heart Association Council on Basic Cardiovascular Sciences CoCC, Council on Functional G Translational B. Animal models of heart failure: A scientific statement from the american heart association. Circ Res. 2012; 111:131–150. [PubMed: 22595296]
51. Mann DL, Bristow MR. Mechanisms and models in heart failure: The biomechanical model and beyond. Circulation. 2005; 111:2837–2849. [PubMed: 15927992]
52. Jessup M, Brozena S. Heart failure. N Engl J Med. 2003; 348:2007–2018. [PubMed: 12748317]
53. Eichhorn EJ, Bristow MR. Medical therapy can improve the biological properties of the chronically failing heart. A new era in the treatment of heart failure. Circulation. 1996; 94:2285–2296. [PubMed: 8901684]
54. Sutton MG, Sharpe N. Left ventricular remodeling after myocardial infarction: Pathophysiology and therapy. Circulation. 2000; 101:2981–2988. [PubMed: 10869273]
55. Prabhu SD, Chandrasekar B, Murray DR, Freeman GL. Beta-adrenergic blockade in developing heart failure: Effects on myocardial inflammatory cytokines, nitric oxide, and remodeling. Circulation. 2000; 101:2103–2109. [PubMed: 10790354]
56. van de Wal RM, Plokker HW, Lok DJ, Boomsma F, van der Horst FA, van Veldhuisen DJ, van Gilst WH, Voors AA. Determinants of increased angiotensin ii levels in severe chronic heart failure patients despite ace inhibition. International journal of cardiology. 2006; 106:367–372. [PubMed: 16337046]
57. MacFadyen RJ, Lee AF, Morton JJ, Pringle SD, Struthers AD. How often are angiotensin ii and aldosterone concentrations raised during chronic ace inhibitor treatment in cardiac failure? Heart. 1999; 82:57–61. [PubMed: 10377310]

58. Swedberg K, Eneroth P, Kjekshus J, Wilhelmsen L. Hormones regulating cardiovascular function in patients with severe congestive heart failure and their relation to mortality. Consensus trial study group. Circulation. 1990; 82:1730–1736. [PubMed: 2225374]

59. Ferrario CM, Flack JM. Pathologic consequences of increased angiotensin ii activity. Cardiovascular drugs and therapy / sponsored by the International Society of Cardiovascular Pharmacotherapy. 1996; 10:511–518. [PubMed: 8950064]

60. Rocha R, Chander PN, Zuckerman A, Stier CT Jr. Role of aldosterone in renal vascular injury in stroke-prone hypertensive rats. Hypertension. 1999; 33:232–237. [PubMed: 9931110]

Novelty and Significance

What Is Known?

- Renin-angiotensin aldosterone system (RAAS) activation in congestive heart failure (CHF) is associated with skeletal muscle wasting.
- RAAS inhibition reduces cachexia in CHF patients.
- Angiotensin II (Ang II) induces skeletal muscle atrophy via ubiquitin proteasome system (UPS) induction via the E3 ubiquitin ligase muscle RING-finger (MuRF) 1.

What New Information Does This Article Contribute?

- We show that Ang II increases *MuRF1* expression and mediates skeletal muscle wasting.
- The novel pathway regulates the lysosomal hydrolase-coordinating transcription factor EB (TFEB) via histone deactylase-5 (HDAC5) and protein kinase D1 (PKD1).
- TFEB influences not only lysosomal and autophagosomal, but also UPS-dependent protein degradation.

Muscle wasting often occurs in patients with advanced stages of heart failure and worsens prognosis. RAAS activation with increased Ang II is implicated. Ang II increases muscular protein degradation through increased *MuRF1* expression. This muscle-enriched E3 ubiquitin ligase is a key mediator of muscle atrophy. However, the Ang II-dependent signaling pathway was unknown. We report that TFEB regulates *MuRF1* expression and thereby UPS-dependent protein degradation. Recently, TFEB was shown to regulate biogenesis of lysosomes and autophagosomes in non-muscle tissue. We show that TFEB directly binds to the *MuRF1* promoter. Ang II/PKD1/HDAC5 signal transduction pathway controls TFEB activity. TFEB inhibition abolished Ang II-induced atrophy in vitro. Likewise, myocyte-specific *PKD1* deletion attenuated Ang II-induced atrophy in mice in vivo. Our study provides evidence for novel signaling downstream of Ang II that mediates Ang II-induced skeletal muscle wasting. We conclude that TFEB serves as a nodal transcription factor not only regulating lysosomal and autophagosomal, but also UPS-dependent protein degradation. The PKD1/HDAC5/TFEB/MuRF1 axis could constitute a potential therapeutic avenue to attenuate Ang II-mediated muscle wasting disorders.

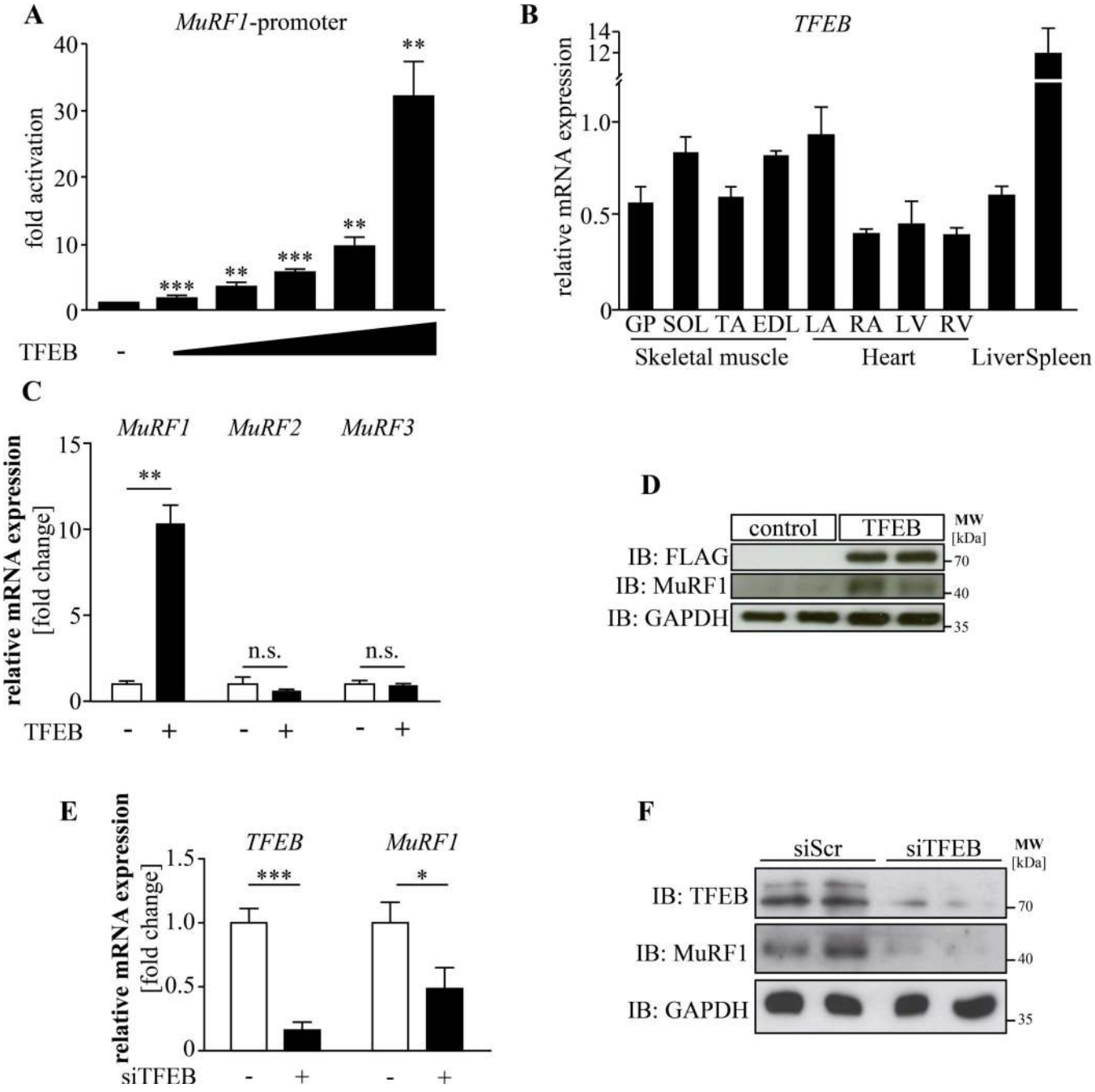

Figure 1. A cDNA expression screen identified the transcription factor EB (TFEB) as activator of the human MuRF1 promoter

(**A**) Luciferase assays performed on cell extracts of COS-7 cells transfected with Hs_*MuRF1*-Luc (−543 bp) with increasing amounts of FLAG-TFEB (TFEB) or empty (−) plasmid. Luciferase activity was normalized to expression of CMV-LacZ and expressed as fold-increase. Data are represented as mean ± SD. **P<0.005, ***P<0.001. (**B**) qRT-PCR analysis of *TFEB* expression in skeletal muscle, heart, liver and spleen of C57Bl6/N mice (n = 4–5). *GAPDH* expression was used as reference. Data are represented as mean ± SD. GP indicates gastrocnemius/plantaris, Sol, soleus; TA, tibialis anterior, EDL, extensor digitorum

longus; LA, left atrium; RA, right atrium; LV, left ventricle; RV, right ventricle. (**C**) qRT-PCR of *MuRF1*, *MuRF2* and *MuRF3* expression following transfection of cDNA expression plasmids encoding for FLAG-TFEB (+, TFEB) or empty (−) expression plasmid in C2C12 myoblasts for 24 h. *GAPDH* expression was used as reference. Data are represented as mean ± SD. **P<0.005. n = 3 each. (**D**) C2C12 cells were transfected with expression plasmids encoding wild type FLAG-TFEB (TFEB) or empty (control) expression plasmid for 24h, as indicated. Immunoblotting (IB) with anti-FLAG, anti-MuRF1 or anti-GAPDH antibody was performed. (**E, F**) C2C12 myoblasts were transfected with scrambled control siRNA (siScr, −) or siRNA targeting TFEB (siTFEB, +, 100 nM each) for 24h. (**E**) qRT-PCR analysis was performed to measure *TFEB* and *MuRF1* expression. *GAPDH* expression was used as reference. Data are represented as mean ± SD. *P<0.05, ***P<0.001. n = 3 each. (**F**) Western blot analysis was performed with anti-TFEB, anti-MuRF1 or anti-GAPDH antibody.

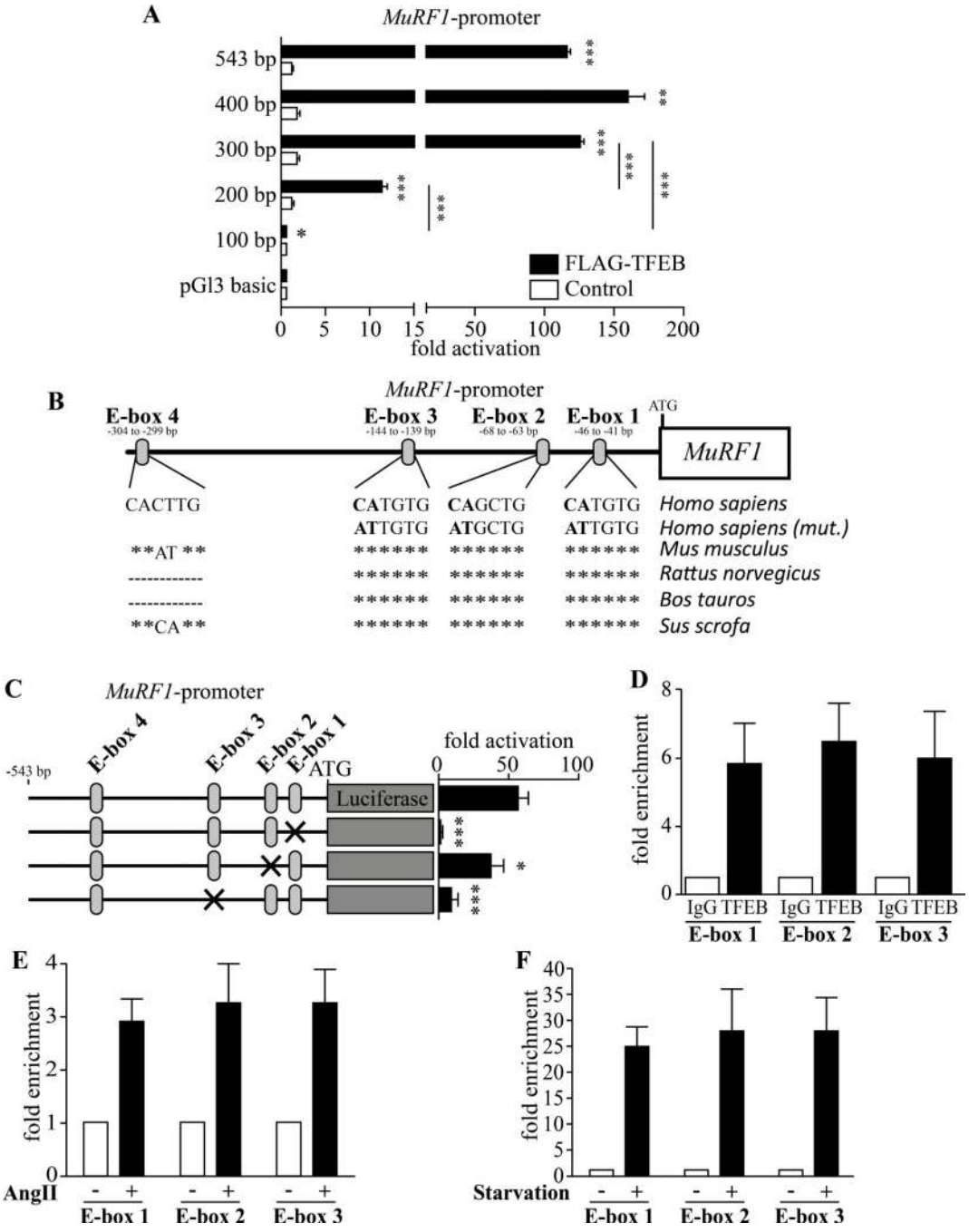

Figure 2. TFEB regulates *MuRF1* expression via conserved E-box elements

(**A**) COS-7 cells were transfected with wild type FLAG-TFEB expression plasmid or empty vector control (control), along with *MuRF1*-promoter constructs, as indicated. Data are represented as mean ± SD. *P<0.05, **P<0.01, ***P<0.005. (**B**) Schematic diagram of the human *MuRF1*-promoter. Positions of conserved E-box motifs (CANNTG) in the *MuRF1*-promoter relative to the transcription start (ATG) are indicated. Alignment shows genomic homology of individual E-box motifs between indicated species. Homo sapiens (mut.) indicates mutated nucleotides to inactivate individual E-boxes (mutated nucleotides are

shown in bold). * indicates homology. (**C**) COS-7 cells were transfected with a TFEB expression plasmid and the indicated *MuRF1*-promoter constructs (−543 bp) harboring E-box mutations as shown in (B). Data are represented as mean ± SD. *P<0.05, ***P<0.005. (**D**) Chromatin immunoprecipitation (ChIP) assay performed on chromatin from C2C12 myoblasts using antibodies against TFEB. Primers flanking E-boxes 1, 2 and 3 of the *MuRF1*-promoter were used. Values indicate the fold-enrichment over chromatin immunoprecipitated with antibodies against IgG. n=5. (**E, F**) ChIP assay performed on chromatin from angiotensin II (Ang II, +) and vehicle treated (−) C2C12 myoblasts (**E**). ChIP assay performed on chromatin from serum starved (+) and untreated (−) C2C12 myoblasts (**F**). Chromatin was immunoprecipitated with antibodies against TFEB. Antibodies against IgG were used as control. n=3.

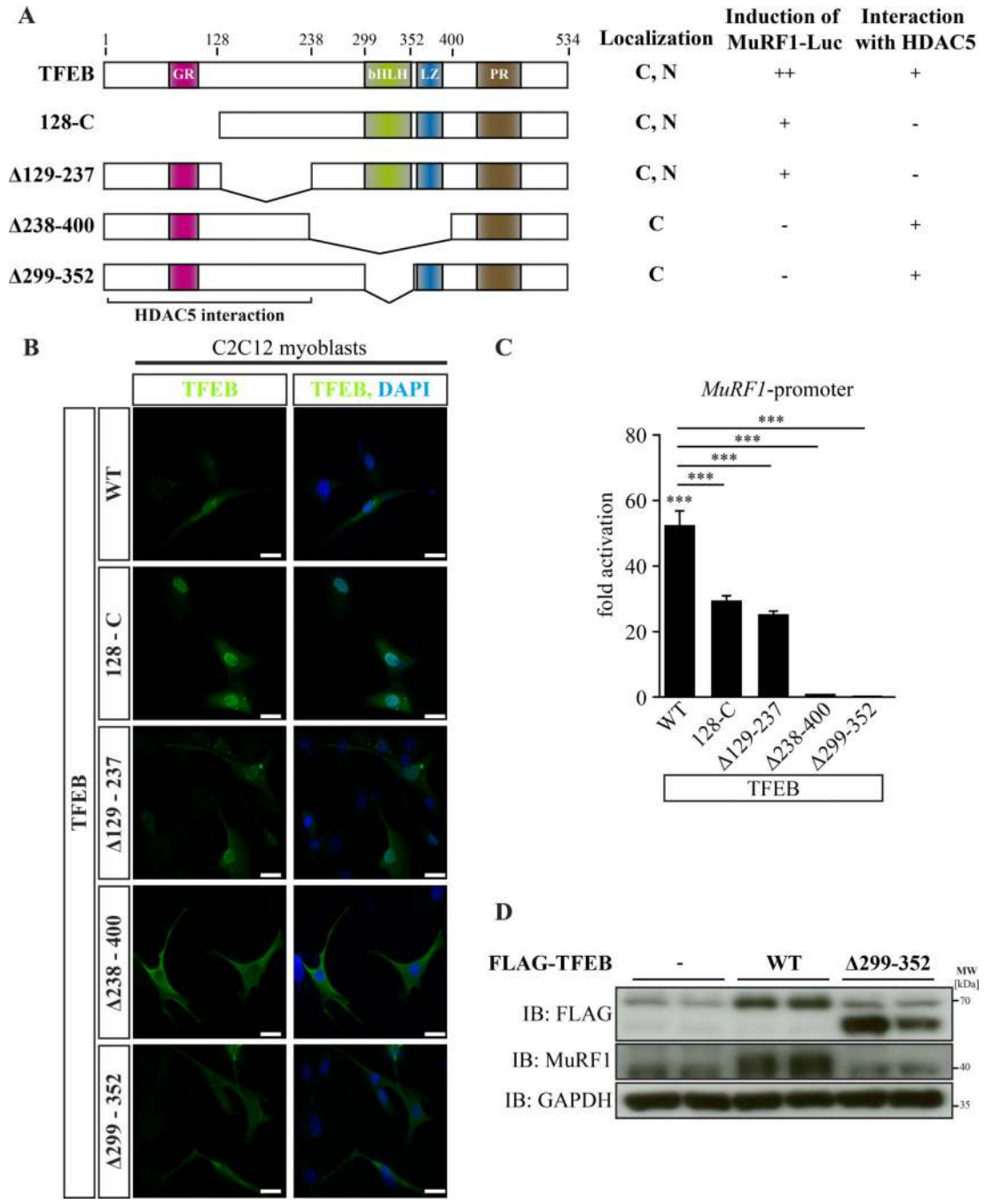

Figure 3. Induction of *MuRF1* expression is mediated through TFEB's bHLH domain

(**A**) Schemes of wild type TFEB and its deletion mutants used in this study. The presence of wild type and mutant TFEB protein in the nucleus (N) or cytoplasm (C), as detected by immunostaining, their ability to induce *MuRF1* expression in luciferase assays, or their interaction with HDAC5 in coimmunoprecipitation assays, respectively, are indicated. GR indicates glycine-rich domain; bHLH, basic Helix-Loop-Helix domain; LZ, Leucine Zipper domain; PR, Proline-rich domain. (**B**) The subcellular distribution of wild type FLAG-TFEB and its deletion mutants in transfected C2C12 myoblasts was detected by

immunofluorescence using anti-TFEB antibody together with A488-coupled secondary antibody. Nuclei were stained with DAPI (blue); scale bar 20 μm. (**C**) HEK293 cells were transfected with the Hs_*MuRF1*_Luc reporter construct (−543 bp) and expression plasmids encoding wild type or mutant TFEB, as indicated. Luciferase activity was normalized to expression of CMV-LacZ and calculated as fold-increase. Data are represented as mean ± SD.*P<0.05; ***P<0.001. n = 3. (**D**) C2C12 cells were transfected with expression plasmids encoding wild type (WT) FLAG-TFEB, TFEB deletion mutant Δ299–352 or empty expression plasmid (control) for 24 h, as indicated. Immunoblotting (IB) with anti-FLAG, anti-MuRF1 or anti-GAPDH antibody was performed.

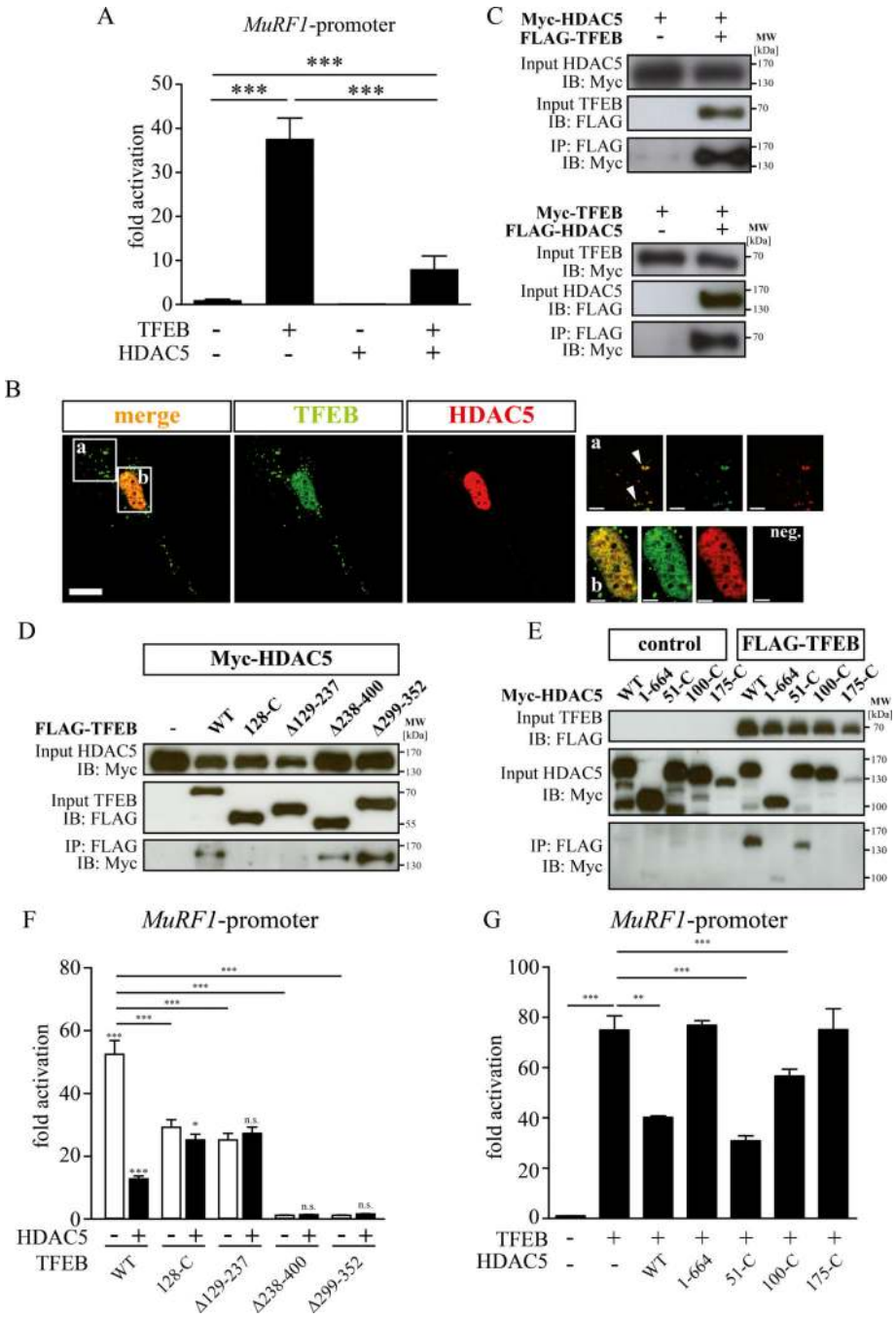

Figure 4. TFEB induced *MuRF1* expression is inhibited by HDAC5

(**A**) HEK293 cells were transfected with *MuRF1*-luciferase reporter (−543 bp) and expression plasmids encoding wild type TFEB, histone deacetylase (HDAC) 5 or empty vector control as indicated. Data are represented as mean ± SD. ***P<0.001. n = 3. (**B**) The subcellular distribution of wild type TFEB-GFP and HDAC5-Myc in transfected C2C12 myoblasts was detected by immunofluorescence. (a + b) indicate augmentations. neg. = negative control. (**C**) Co-IP with lysates from HEK293 cells expressing Myc-HDAC5 and FLAG-TFEB (top panel), or TFEB-Myc(His)$_6$ and FLAG-HDAC5 (bottom panel), as

indicated. Extracts were immunoprecipitated (IP) with anti-FLAG antibody and detected with an antibody directed against Myc. Input proteins were detected by Western blot (IB) with anti-FLAG and anti-Myc antibodies, respectively. n = 5. (**D**) Co-IP assay with lysates from HEK293 cells expressing wild type FLAG-TFEB or TFEB deletion mutants along with wild type Myc-HDAC5, as indicated. IP of TFEB-fusion proteins were using anti-FLAG antibody and detection by anti-Myc antibody. Input proteins were detected by Western blot (IB) with antibodies directed against FLAG and Myc. n = 3. (**E**) Co-IP assay with lysates from HEK293 cells expressing wild type Myc-HDAC5 or HDAC5 deletion mutants along with wild type FLAG-TFEB, as indicated. TFEB-fusion proteins were immunoprecipitated (IP) with anti-FLAG antibody and detected with an antibody directed against Myc. Input proteins were detected by immunoblot (IB) with antibodies directed against FLAG and Myc. n = 3. (**F**) HEK293 cells were transfected with the Hs_*MuRF1*_Luc reporter construct (−543 bp) and expression plasmids encoding wild type TFEB, TFEB deletion mutants and wild type HDAC5 as indicated. Data are represented as mean ± SD. **P<0.01, ***P<0.005. n = 3. (**G**) HEK293 cells were transfected with the Hs_*MuRF1*_Luc reporter construct (−543 bp) and expression plasmids encoding wild type TFEB, wild type HDAC5 and HDAC5 deletion mutants. Data are represented as mean ± SD. **P<0.01, ***P<0.005. n = 3.

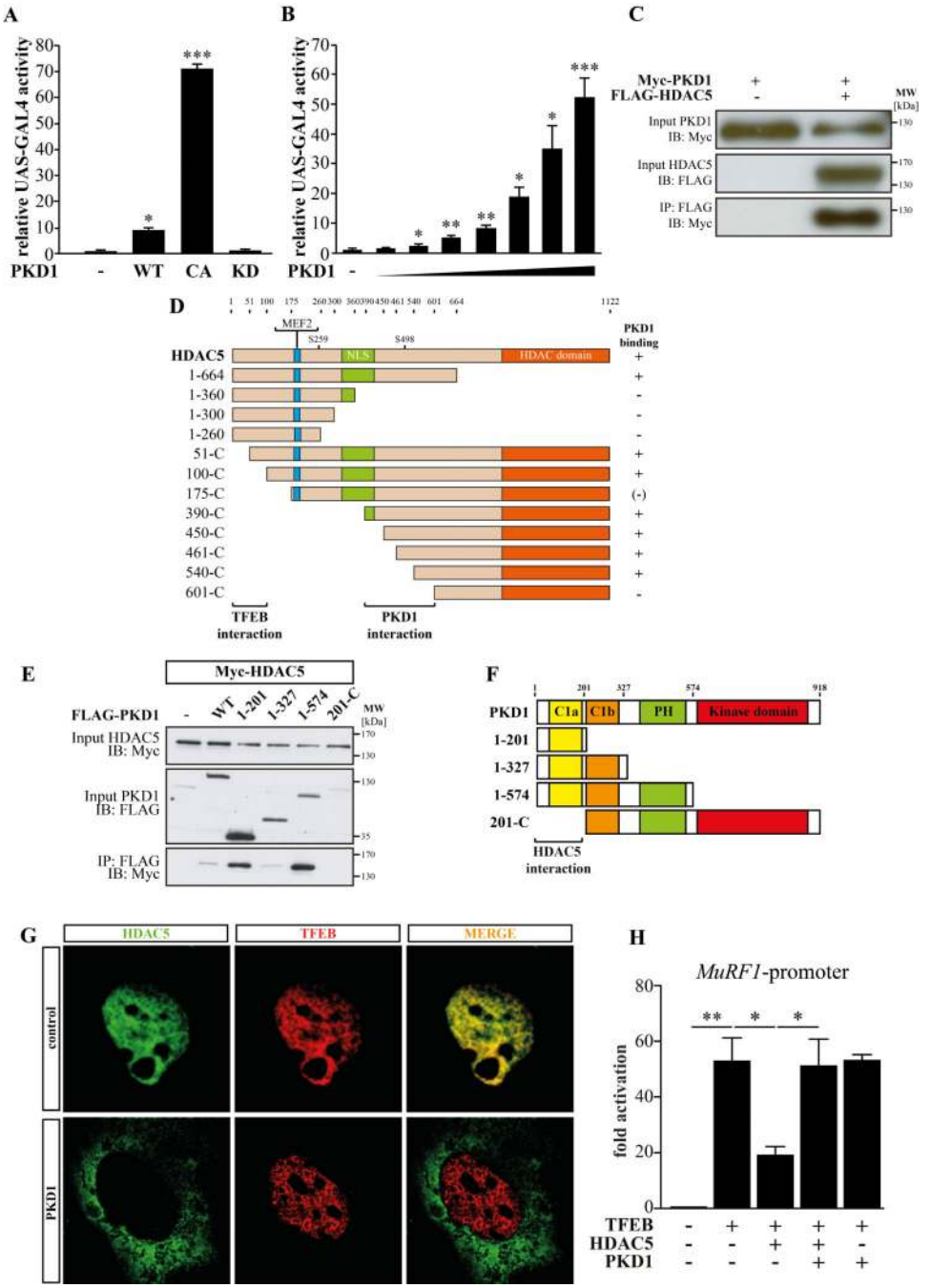

Figure 5. PKD1 relieves HDAC5-mediated TFEB repression

(**A**) HEK293 cells were transfected with UAS-luciferase and expression plasmids encoding GAL4 fused to the wild type HDAC5 N-terminal extension together with 14-3-3-VP16 and expression plasmids of wild type (WT), constitutive active (CA) or kinase inactive (KD) PKD1 as indicated. Values were normalized to expression of CMV-LacZ and calculated as fold-increase. Data are represented as mean ± SD. *P<0.05; ** P<0.005. n = 3. (**B**) HEK293 cells were transfected with UAS-luciferase and expression plasmids encoding GAL4 fused to the wild type HDAC5 N-terminal extension together with 14-3-3-VP16 and increasing

amounts of expression plasmids of PKD1 CA (from 6.25 ng to 400 ng), as indicated. Values were normalized to expression of CMV-LacZ and calculated as fold-increase. Data are represented as mean ± SD. *P<0.05, **P<0.01, ***P<0.005. n = 3. (**C**) Coimmunoprecipitation assay with lysates from COS-7 cells expressing Myc-PKD1 and FLAG-HDAC5, as indicated. HDAC5-fusion proteins were immunoprecipitated (IP) with anti-FLAG antibody and PKD1-fusion proteins were detected with an antibody directed against Myc. Input proteins were detected by Western blot (IB) with antibodies directed against the FLAG or Myc tag. n=3. (**D**) Based on the coimmunoprecipitation data, amino acids 360 to 601 of HDAC5 were identified to be required for physical interaction with PKD1 and, therefore, define a PKD1 binding site. (**E**) Coimmunoprecipitation assay of FLAG-PKD1 deletion mutants coexpressed with Myc-HDAC5 to identify the HDAC5 binding domain of PKD1. PKD1-fusion proteins were immunoprecipitated (IP) with anti-FLAG antibody and HDAC5-fusion proteins were detected with an antibody directed against Myc. Input proteins were detected by Western blot (IB) with antibodies directed against the FLAG or Myc tag. n = 3. (**F**) Based on the coimmunoprecipitation data, amino acids 1 to 201 of PKD1 were identified to be required for physical interaction with HDAC5 and, therefore, define a HDAC5 docking site. Positions of cysteine rich region 1a (C1a, yellow), C1b (orange), pleckstrin homology domain (PH; green) and kinase domain (red) of PKD1 are depicted. (**G**) COS-7 cells were transfected with GFP-HDAC5 and FLAG-TFEB together with an empty vector (pcDNA_3.1) or constitutive active PKD1. Immunostaining was performed with anti-FLAG and anti-GFP antibody. (**H**) HEK293 cells were transfected with expression plasmids encoding wild type FLAG-TFEB, HDAC5-Myc, or PKD1 CA proteins, as indicated, together with the Hs_*MuRF1*_Luc reporter construct (−543 bp). Values were normalized to expression of CMV-LacZ and calculated as the fold-increase in luciferase to CMV-LacZ ratio compared to the reporter alone. Data are represented as mean ± SD. *P<0.05; ** P<0.005. n = 5.

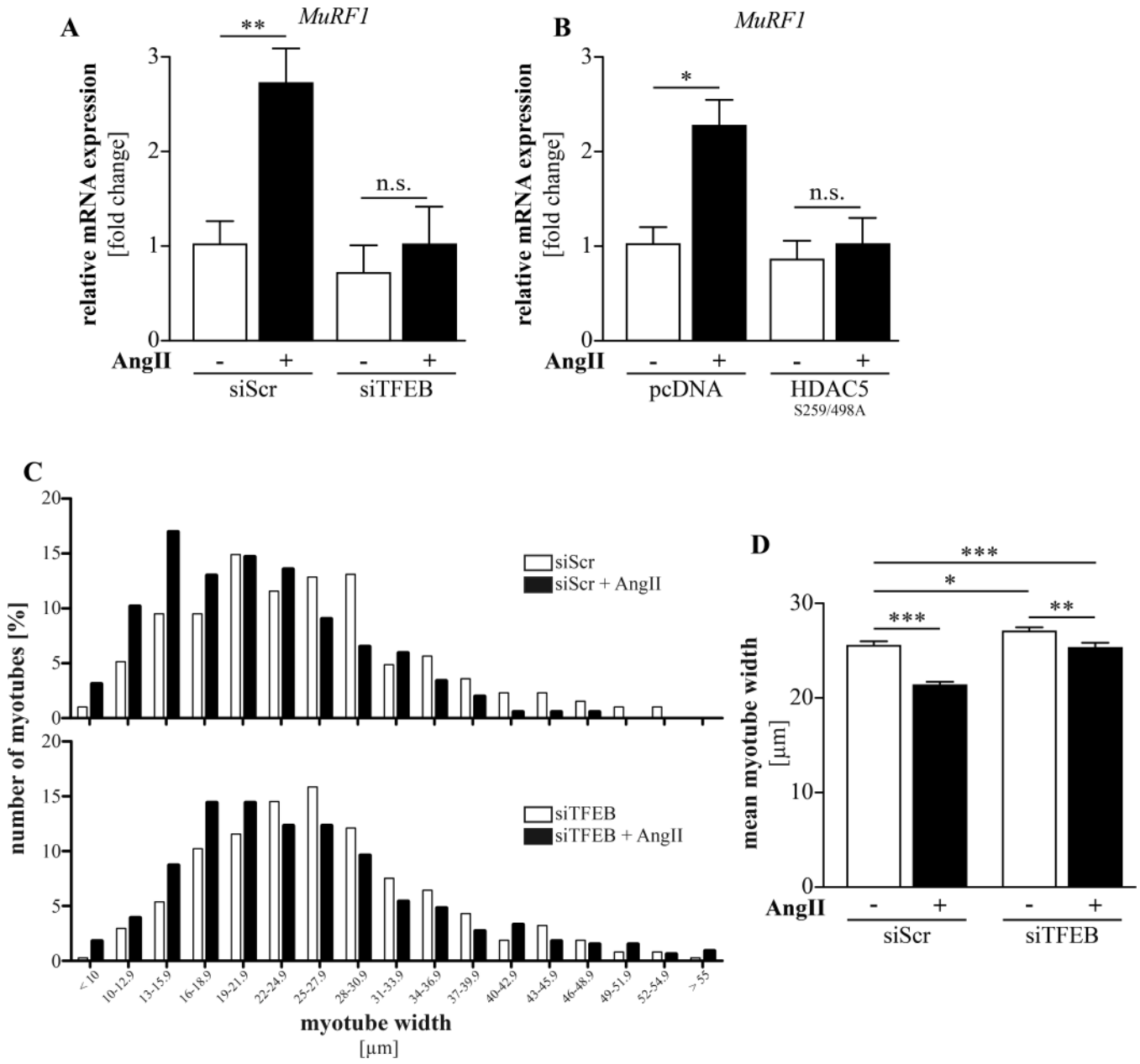

Figure 6. TFEB knockdown reduces endogenous MuRF1 expression and inhibits Ang II induced atrophy of C2C12 myocytes

(**A**) qRT-PCR analysis of MuRF1 expression in C2C12 myotubes following transfection with scrambled control siRNA (siScr) and siRNA targeting TFEB (siTFEB; 100 nM each) for 24h and following treatment with 500 nM Ang II or vehicle (−) for 24 h. GAPDH expression was used as reference. Data are represented as mean ± SEM. **P<0.01. n = 3. (**B**) qRT-PCR analysis of MuRF1 expression in C2C12 myoblasts following transfection with signal-resistant FLAG-HDAC5 S259/498A (harboring alanines in place of serines 259 and 498 which are required for nuclear export of HDAC5). GAPDH expression was used as reference. Data are represented as mean ± SEM. *P<0.05. n = 3. (**C**) C2C12 myoblasts were transfected with scrambled control siRNA (siScr) or siRNA targeting TFEB (siTFEB; 100

nM each), differentiated for 5 days, and treated with 500 nM Ang II or vehicle for 48h. Myotubes were photographed and myotube width was measured using ImageJ software. Number of myotubes belonging to a given range of myotube diameters is shown in a size distribution diagram. (**D**) Changes in mean myotube width following siRNA mediated knockdown of TFEB and Ang II or vehicle treatment is shown. *P<0.05, **P<0.01, ***P<0.005. n = 3 each.

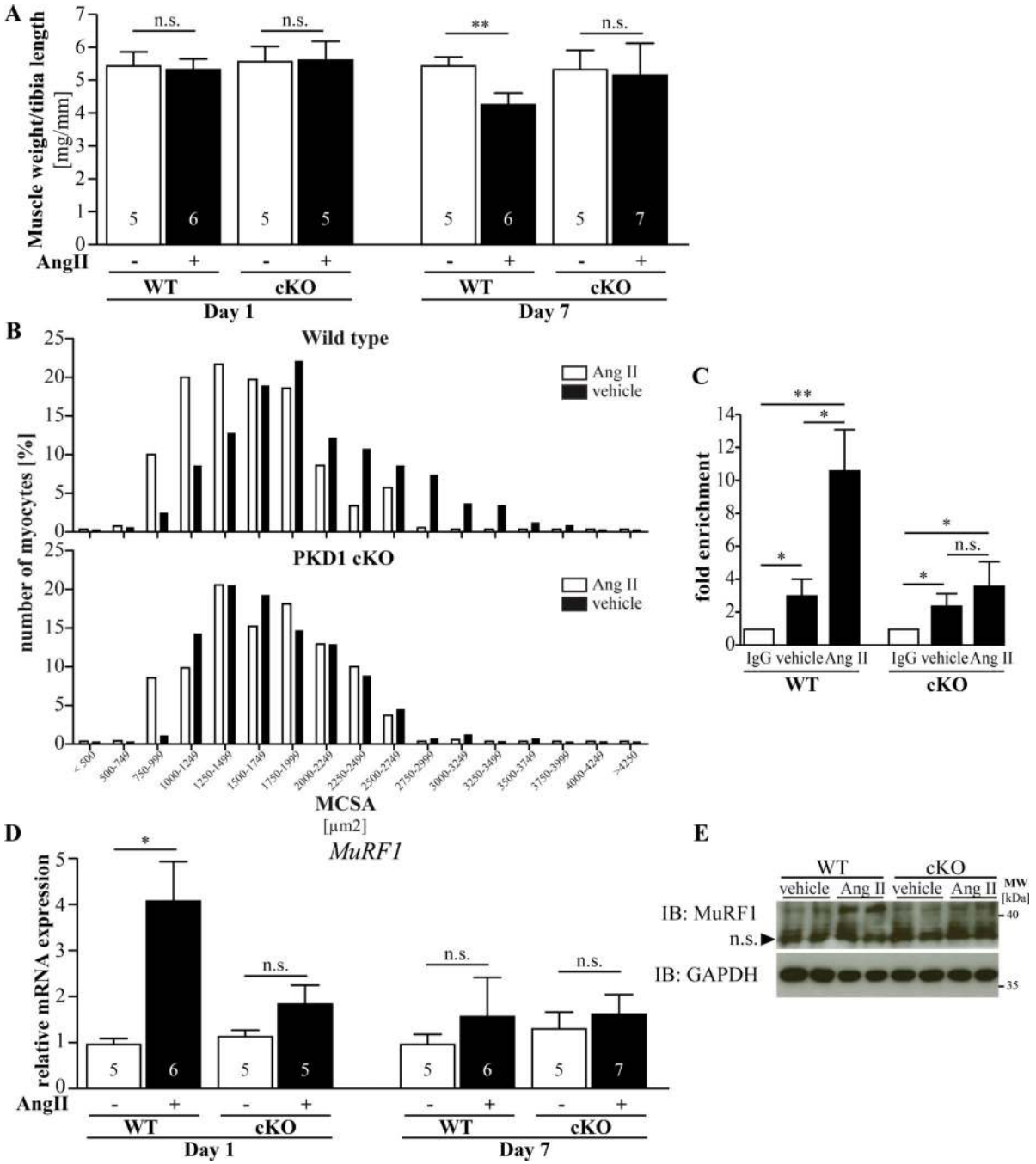

Figure 7. Ang II induced skeletal muscle atrophy is attenuated in PKD1 cKO mice

Ang II (1.5 µg/KG/min) was delivered chronically to 8- to 10-wk-old male PKD1 wild type (WT; $PKD1^{WT/WT;\ MCK\text{-}CRE}$) and skeletal muscle loss of function $PKD1^{loxP/loxP;\ MCK\text{-}CRE}$ (cKO) mice for 24h and 7 days, respectively, by using an implanted osmotic minipump. Vehicle treated wild type ($PKD1^{WT/WT;\ MCK\text{-}CRE}$) and cKO mice were used as controls. Numbers of animals used are indicated. (**A**) *Gastrocnemius/plantaris* to tibia length ratios are shown. **P<0.01. n.s. not significant. (**B**) Myocyte cross sectional area (MCSA) of histological sections from *gastrocnemius/plantaris* (±SEM) of WT and cKO mice after 7

days of Ang II or vehicle treatment. Number of myotubes belonging to the given range of MCSA are shown in a size distribution diagram. (**C**) Chromatin immunoprecipitation (ChIP) assay performed on chromatin from *gastrocnemius/plantaris* of 24h Ang II and vehicle treated WT and cKO mice using anti-TFEB antibody. Primers flanking E-box 1 of the *MuRF1* promoter were used. Values indicate the fold-enrichment over chromatin immunoprecipitated with anti-IgG antibody. n=3. *P<0.05, **P<0.01, n.s. not significant. (**D**) MuRF1 expression in *gastrocnemius/plantaris* (±SEM) of WT and cKO mice after 24h and 7 days of Ang II or vehicle treatment. *GAPDH* was used as a reference. Data are presented as mean±SEM. *P<0.05. (**E**) Western blot analysis on protein lysates from *gastrocnemius/plantaris* of 24h Ang II and vehicle treated WT and cKO mice using anti-MuRF1 and anti-GAPDH antibody. n.s., no specific signal.

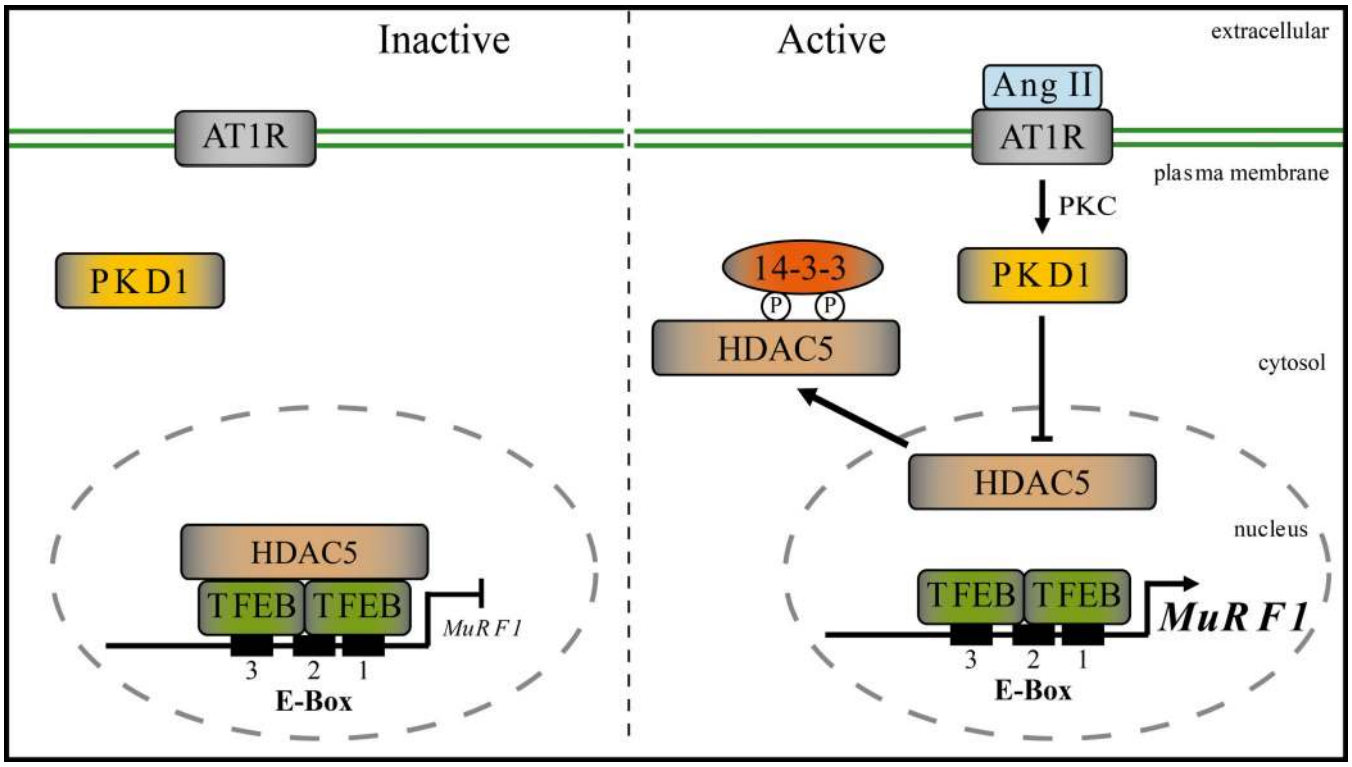

Figure 8. The Ang II/PKD1/HDAC5 signaling pathway regulates TFEB-induced *MuRF1* expression

The PKD1/HDAC5/TFEB/MuRF1 axis mediates Ang II induced skeletal muscle atrophy. Nuclear TFEB specifically binds to conserved E-box motifs in the *MuRF1* promoter localized close to its transcription start site. PKD1 together with HDAC5 controls TFEB activity at the MuRF1 promoter. Inhibition of this signaling pathway could be important to combat Ang II associated muscle wasting disorders such as cardiac cachexia.